Available online at www.CivileJournal.org

Civil Engineering Journal

Vol. 6, No. 10, October, 2020

Evaluation of Seismic Performance of Steel Lattice Transmission Towers

Uğur Albayrak [a*], Loai Morshid [a]

[a] *Department of Civil Engineering, Eskisehir Osmangazi University, Eskisehir, Turkey.*

Received 05 May 2020; Accepted 26 August 2020

Abstract

The electricity transmission systems are an important lifeline for modern societies. They are used for overhead power lines as supporting structures. Transmission towers are designed to meet electrical and structural requirements. They are designed according to the weight of conductors and environmental effects such as wind and ice loads. They also considered other extraordinary stresses such as cable breakage and ice-breaking effects. Because of a common perception that transmission line (TL) towers show low sensitivity to earthquakes, the effects of the earthquake in TL tower construction are not considered. For this reason, TL towers are investigated with regard to the seismic performance in this study. The principal objectives of this research are: i) to assess the sensitivity of typical TL towers to earthquake loads, ii) to retrofit an existing steel lattice tower using a new section Centre To Center (CTC). In this study, a finite element model of a representative 154 KV transmission tower in Turkey was performed using a set of 10 recorded earthquake ground movements. The four-legged square TL tower has been analyzed and designed for Turkey, Eskisehir seismic zone considering 42.95 m height using finite element (FE) software. Therefore, a new section Centre To Center (CTC) type has been designed and the failed sections have been replaced with a designed section using the SAP2000 section designer. The results show that the load of failure increased after retrofitting. The retrofitting method was effective and easily conducted in fields.

Keywords: Earthquake Damage; Non-linear Dynamic Analysis; Retrofitting; Seismic Evaluation; Transmission Tower.

1. Introduction

A transmission steel tower is a high-rise structure, known as an electricity tower. It used to carry overhead lines [1]. Electrical engineering advancement shows the need to support heavy conductors that led to the current existing towers. Transmission line towers are high rise-structures, the height of well-above the side dimensions. These are space frames made of steel profiles, which have a separate foundation for every leg. The customer sets the elevation of the transmission tower and the engineer designs the overall configuration, element, and connection details.

The power generated in power stations was transmitted via transmission power lines and transported by transmission power line towers. The transmitting power line towers cost 35 to 45% of the overall expenditure of the transmission network. So, the largest economy must be achieved in its design and installation [2]. Despite the advanced sensor technology and seismological academic efforts, earthquakes stay unpredictable.

In Turkey, where most of the total population lives in urban areas, for instance, Eskisehir city, which is in northwestern Turkey, is a quiet active zone. Eskisehir's city center lies in the 2nd and 3rd-degree earthquake zones.

* Corresponding author: albayrak@ogu.edu.tr

http://dx.doi.org/10.28991/cej-2020-03091600

The experience of powerful earthquakes in populated areas will have major catastrophic consequences of damage to buildings and residential areas. The physical damage of earthquakes to structures causes minor effects, for example, power, water, or gas outages. Most times, the secondary impact causes more socioeconomic losses than losses from straight structural damage [3].

For the indispensable dependence on electricity in modern society, transmission networks must cover many regions [4]. The ultimate tested capacity is crucial to power transmission systems that is recognized in society as lifeline construction [5]. In the designing stage of a transmission tower, we consider wind loads to be the controlling side load which overrides a load of earthquakes since the transmission tower is in principle light structures. For instance, the National Electrical Safety Code (2012) and in the United States ASCE guidelines (2009) demand the wind impact to be taken into consideration in the design, instead of the earthquake effect.

Therefore, the cross-section of structural elements is determined by taking into account the weight of the tower, the tension in the transmission cable, and the wind load. Despite that, we have noticed that the transmission tower is exposed to severe earthquakes [6]. The lateral displacement of transmission towers, which can be defined as a tall structure, should be limited to acceptable levels under seismic loads. It is essential to have an excellent understanding of the transmission tower's seismic vulnerability to show proper earthquake management [7]. The primary goal will offer a more comprehensive understanding of performing lattice steel transmission towers under earthquake load.

We organize the paper as follows; in Section 2 we present the literature review and a brief discussion of several earlier studies. Section 3 describes the method used in this article, the structural features of the transmission line tower that are selected to study, the selection method of ground motion records, and the nonlinear time-history analysis conducted to find the ability of the tower under earthquake ground motions. Section 4 presents a design using AISC360-16 and the failed sections replacement with a designed section. In the last section, we discuss the results.

2. Scientific Literature Review

In response to that mentioned in the Introduction, extensive investigations have been carried out in recent decades to study the seismic performances of transmission tower systems, including analytical, experimental [8], and numerical [9] studies. An alternative model of material that can recognize the non-linear behavior of steel members, when axial cyclic loads applied, was developed further in [10] and applied to stimulate the ongoing failure of TL towers during earthquakes [11]. However, the limited studies [12] have aimed to study the seismic risk evaluation of the TL tower. Wu and Pantelides (2019) carried out a study that presents the seismic evaluation of deficient bridge bent under nonlinear static and dynamic analysis in which a nonlinear time history analysis was conducted in the study to evaluate the seismic performance. The research shows that the method used for the repair of RC bridge bents was effective [13].

Moon et al. (2009) performed a semi-scaled substructure test to assess the behavior and the fault position of an existed transmission tower exposed to wind loads. He observed from the experiment that local regional buckling occurred on the two legs elements where they had been exposed to compression. To avoid associated regional buckling and irregular deformation, the elements must be enlarged or braces must be added to weak joints [14].

Alam and Santhakumar [15] carried out a test of load on a 34-meter elevated transmission tower under a 200 kV capacity. They discovered that the total bending of the tower legs and the transverse components caused the tower to fail. In the results of the tests, they proposed reduction of the highest slenderness ratio of 150 to 110, as stated in the steel transmission tower's design code [16]. We can find few works in the literature of seismic behavior of transmission towers.

Lei and Chien (2009) examined the dynamic behavior of a coupled tower conductor-system during powerful earthquake movements. They implemented a detailed finite-element model of structural towers and the overhead line, taking into account the geometric nonlinearities and the interaction model of a soil-structure in the numerical simulations. The authors stated that neglecting the contribution to overhead lines of the earthquake reaction to support towers would lead to errors in estimating the largest strength of supporting tower elements [17].

Chen et al. (2014) summarized the state-of-the-art on dynamics and control of vibration in transmission tower systems. In the article, they carried out and discussed the investigations into dynamic reactions to transmission line towers under ice, wind, and earthquake load conditions. Considering the seismic behavior of transmission towers, the authors made out the following conclusion: a) The transmission lines spans are large compared to today's civil engineering constructions, so the effects of multiple excitations must be in details; b) The common failure of transmission line tower systems show that the load patterns given in the codes still do not represent extreme load conditions, for example, those resulting from seismic ground movements and the designed method based on them. The static analysis is a restricted and dynamic analysis of the interaction of Tower-line systems [18].

3. Method

3.1. Description of the Structural Model

The selected tower was a suspension (tangent) tower. It is used for straight runs or with a line deviation of 0º to 2º. The model of the tower bracing is a Diamond lattice system as seen in Fig.1. This tower model has been selected because it is one of the most used models. The sections used for the tower are steel angles made from S355 which is a non-alloy European standard (EN 10025-2) structural steel. Fig.2 displays the finite element model of the studied TL system which comprises three towers and four spans of transmission lines. As seen, the system is symmetrical with the middle spans and spans on the side of 400 m and 200 m.

The transmission tower has been modeled on AutoCAD and then imported to SAP2000 (SAP 2000, computer, and structures). We chose this program because of its dynamic analysis capabilities. The transmission tower is fixed at the base. The height of the tower is 42.95 meter and the base width of the tower is 4 meters. Figures 3 and 6, show the geometry of the 154 KV tower.

Figure 1. Images of the transmission tower 154 KV

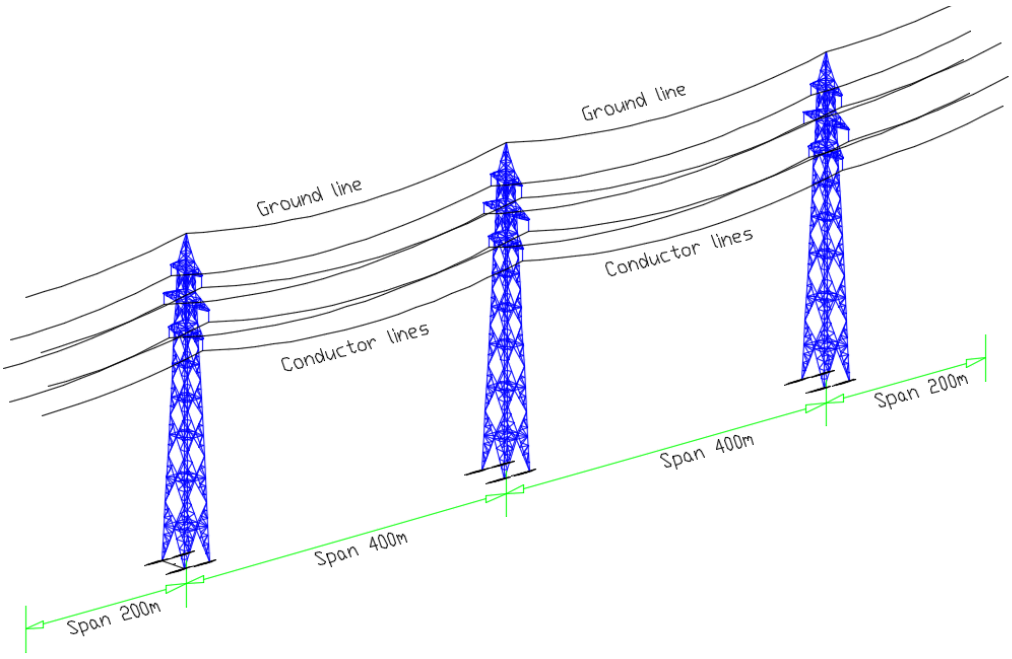

Figure 2. FE model of the transmission tower-line system

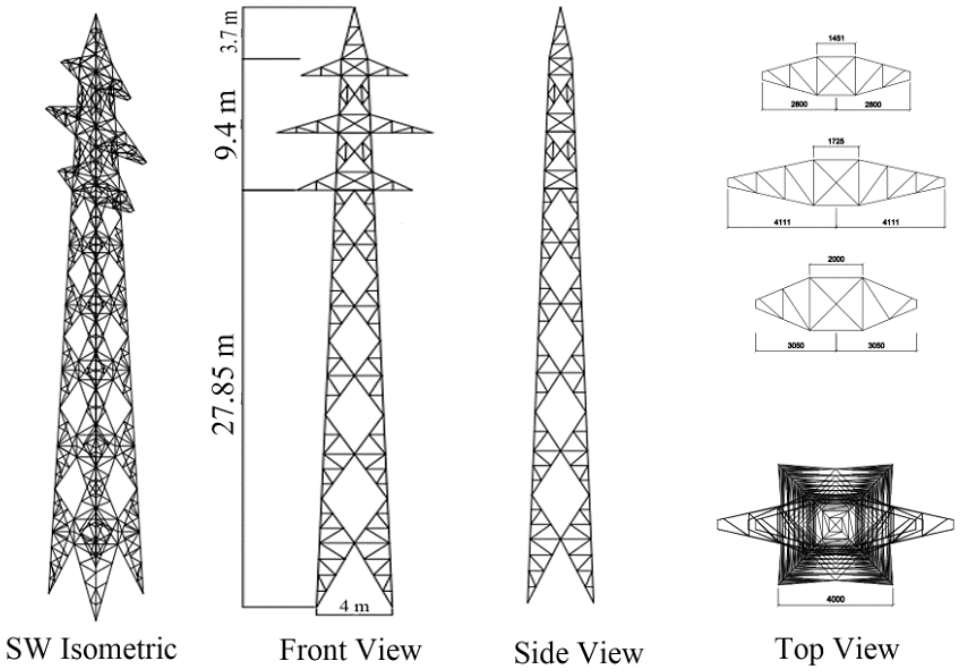

Figure 3. The geometry of 154 kV lattice tower

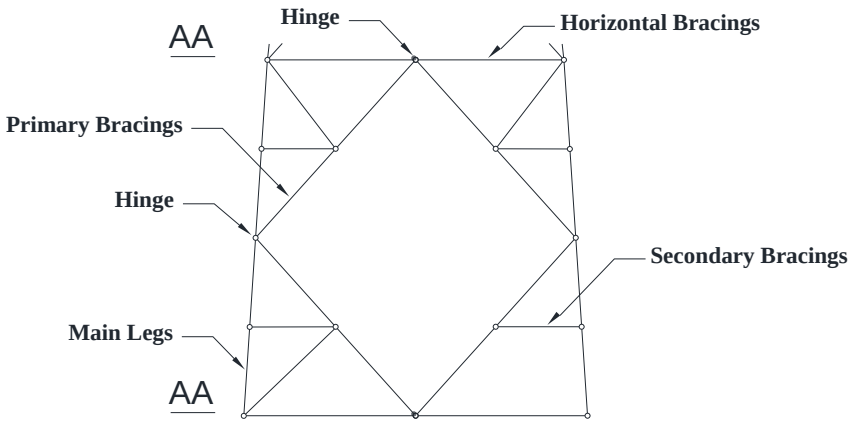

Figure 4. Dummy bars sued in the structure vertical plan [19]

3.2. Steel and Section Profiles

For the aim of this study, the members have been modeled on the size of the profiles and the grade in steel for guaranteed realistic contributions to the dead load on the models. In this study, analysis of steel connections has not been considered, so elements including holes of bolts or bolts have been omitted. Figure 4 shows the Dummy bars used in the vertical plane.

The tower used in this study was modeled with different steel equal angles (L -profile) sizes. Table 1 lists the member sections used in the study. Figure 5 shows instances of L-profile arrangements.

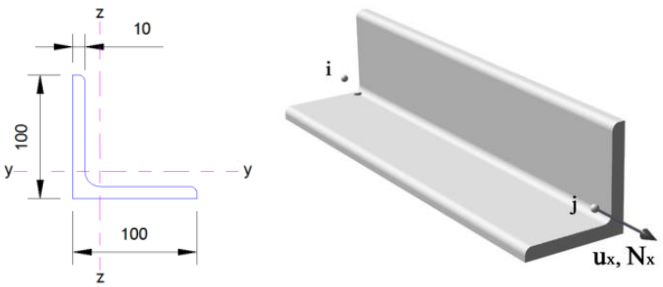

Figure 5. Single angle L100x10 profile

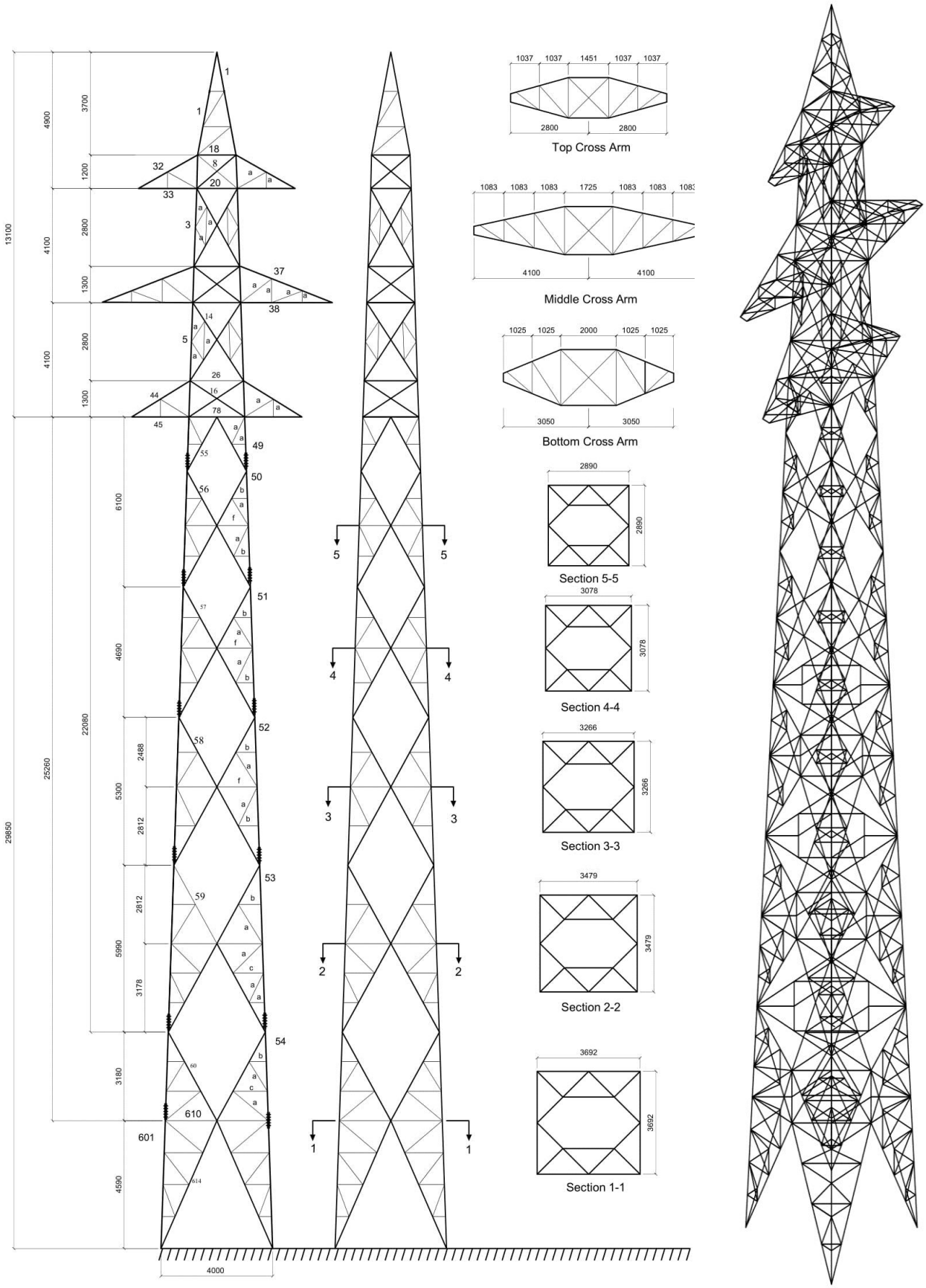

Figure 6. The geometry of 154 kV lattice tower (all units in millimeters)

Table 1. List of member profiles used in the study

Section	No.	Profile size	Unit Weight (Nm^{-1})	Area (mm^2)	Radius of Gyration Rx = Ry (mm)	Ix=Iy (cm^4)	Wx=Wy (cm^3)
Peak legs	1	L60X60X5	44.83	581.9	18.245	19.4	4.45
Cage legs	2	L120X120X11	195.22	2537	36.641	340.6	39.41
	3	L120X120X11	195.22	2537	36.641	340.6	39.41
	4	L120X120X11	195.22	2537	36.641	340.6	39.41
	5	L120X120X11	195.22	2537	36.641	340.6	39.41
	6	L150X150X14	310	4004	46.308	845.4	78.33
Cage Primary Bracing	8	L50X50X5	36.99	480.3	15.106	11	3.05
	10	L80X80X7	83.28	1082	24.355		
	12	L70X70X7	72.50	939.7	21.214	42.4	8.43
	14	L100X100X10	147.54	1900	30.78	177	24.7
	16	L80X80X7	83.28	1082	24.355		
Cage Horizontal Bracing	18	L60X60X5	44.83	581.9	18.245	19.4	4.45
	20	L80X80X7	83.28	1082	24.355		
	22	L70X70X7	72.50	939.7	21.214	42.4	8.43
	24	L100X100X8	119.49	1551	30.555	145	20
	26	L70X70X7	72.46	939.7	21.214		
Top Cross Arm Beams	32	L60X60X5	44.83	581.9	18.245	19.4	4.45
	33	L80X80X10	116.35	1511	24.064	87.7	15.5
Middle Cross Arm Beams	37	L70X70X6	62.69	812.7	21.302	36.9	7.27
	38	L100X100X10	147.54	1915	30.376	177	24.7
Bottom Cross Arm Beams	44	L60X60X6	53.17	684	18.468	22.9	5.25
	45	L80X80X7	83.28	1082	24.355		
Main legs	49	L150X150X14	310.00	4004	46.308	845.4	78.33
	50	L150X150X14	310.00	4004	46.308	845.4	78.33
	51	L180X180X16	426.74	5504	55.681	1682	129.7
	52	L180X180X18	476.77	6191	54.9	1866	144.7
	53	L200X200X18	531.70	6911	61.336	2600	180.6
	54	L200X200X20	587.91	7635	61.107	2854	199.3
	601	L200X200X20	587.91	7635	61.107	2854	199.3
Leg Primary Bracings	55	L120X120X11	195.22	2537	36.641	340.6	39.41
	56	L100X100X12	174.91	2271	30.169	207	29.2
	57	L100X100X10	147.54	1900	30.78	177	24.7
	58	L100X100X10	147.54	1900	30.78	177	24.7
	59	L100X100X8	119.49	1551	30.555	145	20
	60	L100X100X8	119.49	1551	30.555	145	20
	614	L100X100X8	119.49	1551	30.555	145	20
Leg Horizontal Bracing	610	L60X60X5	44.83	625	20.217	19.4	4.45
	510	L70X70X6	62.69	812.7	21.302	36.9	7.27
	410	L60X60X5	44.83	581.9	18.245	19.4	4.45
	310	L70X70X6	62.69	812.7	21.302	36.9	7.27
	110	L80X80X7	83.28	1082	24.355		
Secondary Bracings	a	L35X35X3	15.70	203.7	10.605	2.3	0.9
	b	L40X40X4	23.74	307.9	12.052	4.49	1.55
	c	L45X45X4	26.98	349.3	13.568	6.47	1.97
	d	L50X50X4	30.12	389.3	15.182	9.01	2.47
	e	L50X50X5	36.98	480.3	15.106	11	3.05
	f	L60X60X5	44.83	581.9	18.245	19.4	4.45

3.3. Material Properties

The TL tower designed according to S355 for each structural member has been shown in Table 2.

Table 2. Material properties of S355 steel

Property	Symbol	Unit	Value
Modulus of elasticity	E	(MPa)	210×10^3
Yield strength	F_y	(MPa)	355
Ultimate strength	F_u	(MPa)	510
Poisson's ratio	ν	(-)	0.3

3.4. Load Cases

The loading calculations on the tower, according to the Turkish Standard International Electrical Commission (TS IEC) 60826 standard, and a set of load cases have been taken into consideration for the transmission tower design in this study. This article concerned with static and dynamic earthquake loads applications, so we calculated the load cases involving wind and ice load cases and broken wire conditions.

When defining wind direction, the following terminology was used: transversal for loads which act on the tower side; Longitudinal direction for loads which act on the tower face (in the line's direction); vertical direction for loads that act downwards or upwards. Figure 7 illustrates these terms and conventions.

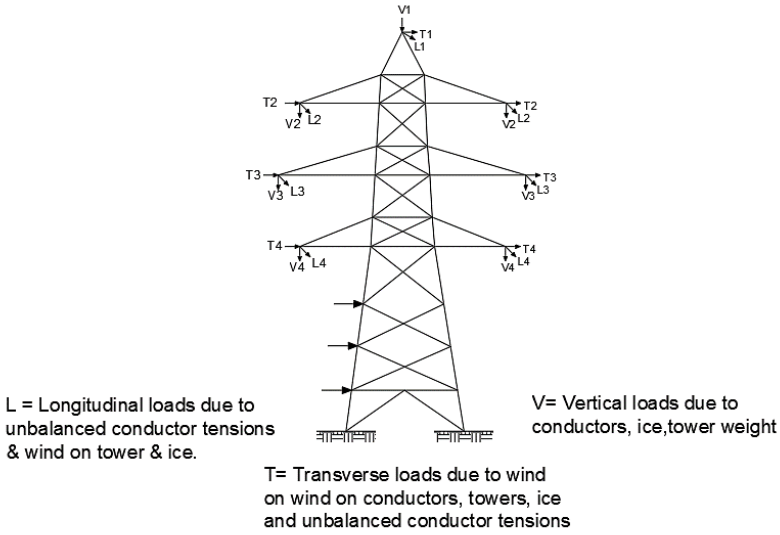

Figure 7. Load direction conventions

In all cases, several load effects on the TL tower have been analyzed to simulate the actual properties of the wind angles and other load cases. Table 3 shows the examined load cases. We have defined the details of the 20 load cases as combinations of different loads as seen in Figure 8.

Table 3. Description of the load cases

Case #	Load case description
1	Unstable loads
2	Unstable loads
3	Right top and middle conductor coupling
4	Right top conductor closing single circuit
5	Right middle and bottom conductor coupling
6	Right middle conductor closing single circuit
7	Right top and bottom conductor coupling

8	Right bottom conductor coupling single circuit
9	Earth wire broken
10	Earth wire broken
11	Even wind
12	One vertical wind single circuit
13	Maximum angle drawing
14	Maximum angle drawing
15	Unbalanced icing
16	Unbalanced icing
17	Down opening
18	Down opening
19	Net up lifting opening
20	Down opening

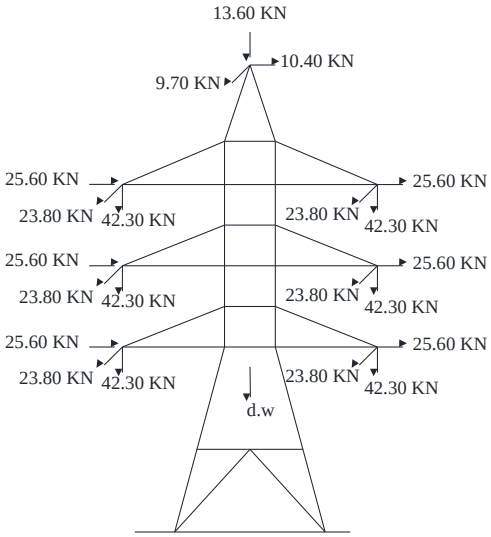

Load case description: 1.UNSTABLE LOADS

Case #: 1

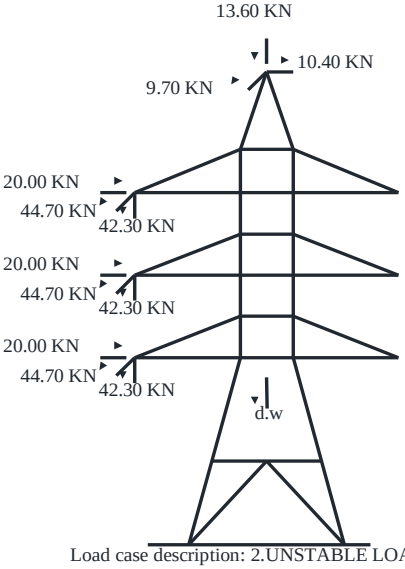

Load case description: 2.UNSTABLE LOADS

Case #: 2

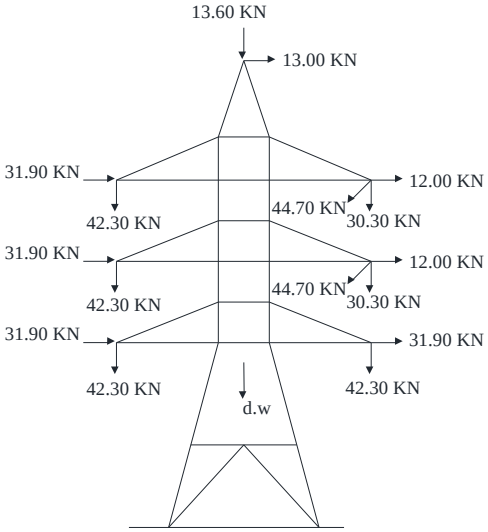

Load case description: RIGHT TOP AND MIDDLE CONDUCTOR COUPLING

Case #: 3

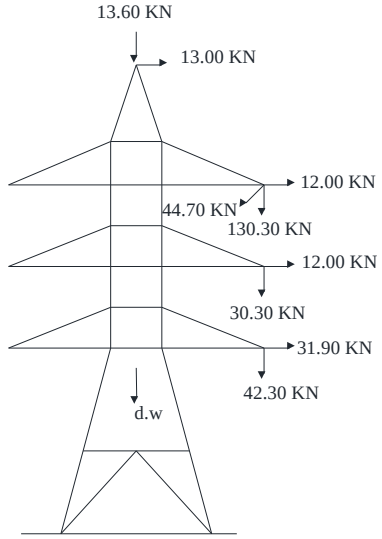

Load case description: RIGHT TOP CONDUCTOR CLOSING SINGLE CIRCUIT

Case #: 4

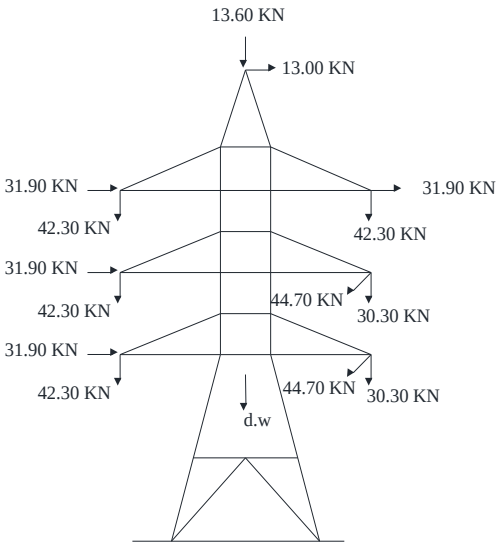

Load case description: RIGHT MIDDLE AND BOTTOM CONDUCTOR COUPLING
Case #: 5

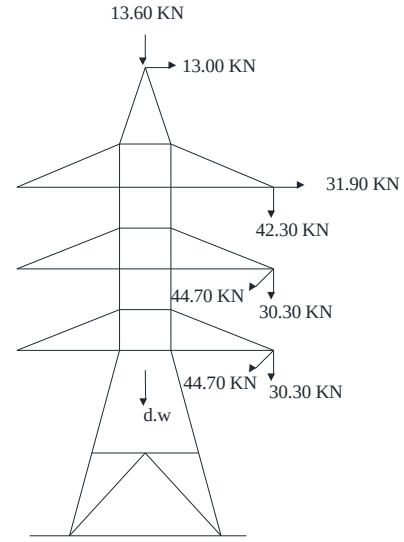

Load case description: RIGHT MIDDLE CONDUCTOR CLOSING SINGLE CIRCUIT
Case #: 6

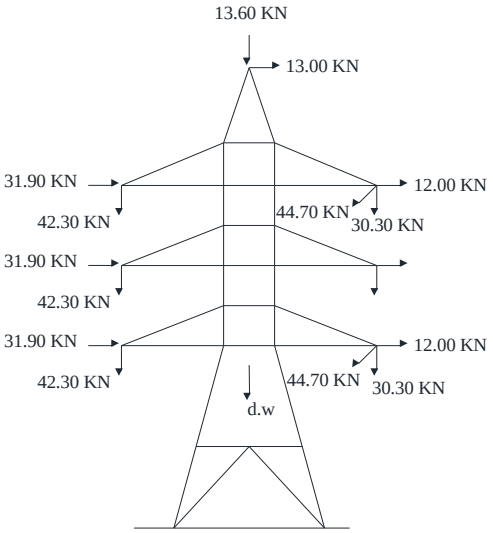

Load case description: RIGHT TOP AND BOTTOM CONDUCTOR COUPLING
Case #: 7

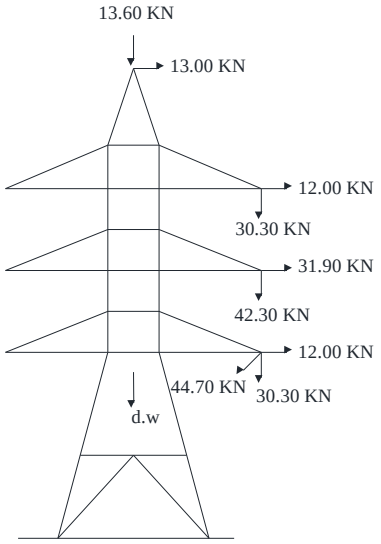

Load case description: RIGHT BOTTOM CONDUCTOR COUPLING SINGLE CIRCUIT
Case #: 8

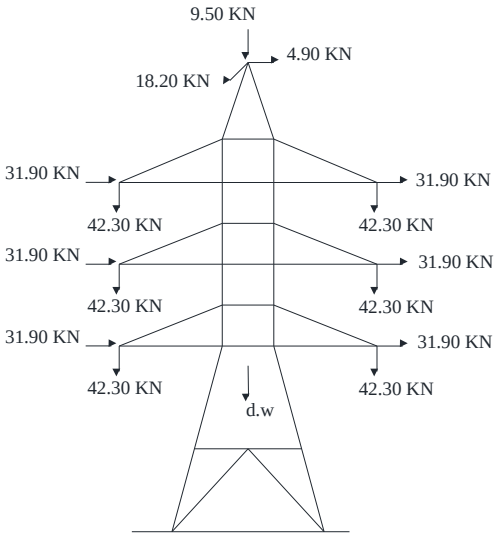

Load case description: 1.EARTH WIRE BROKEN
Case #: 9

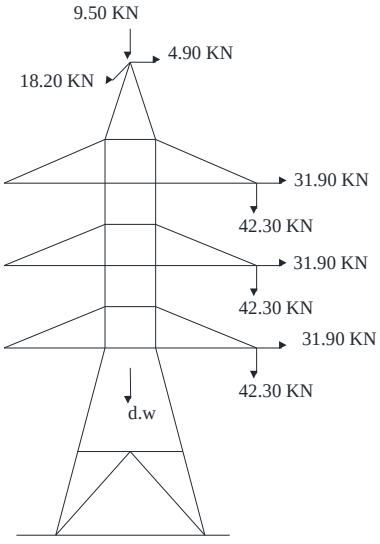

Load case description: 2.EARTH WIRE BROKEN
Case #: 10

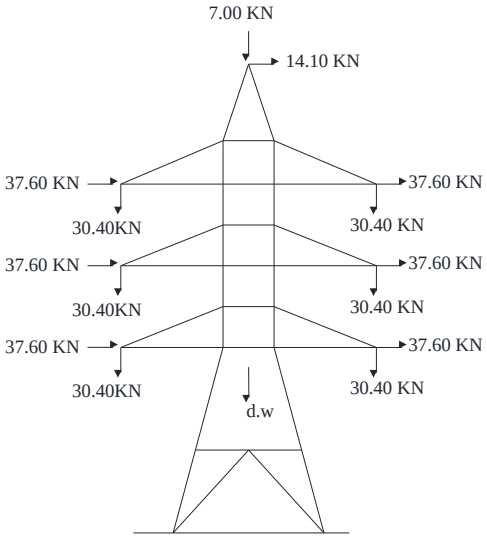

Load case description: EVEN WIND
Case #: 11

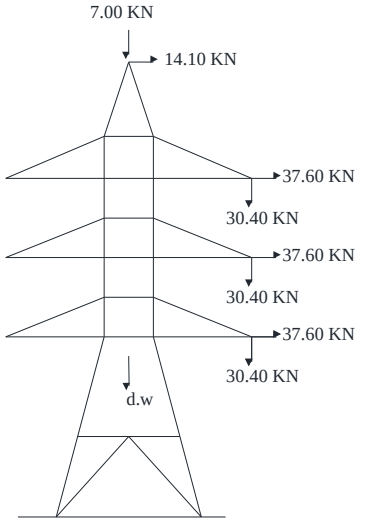

Load case description: ONE VERTICAL WIND SINGLE CIRCUI
Case #: 12

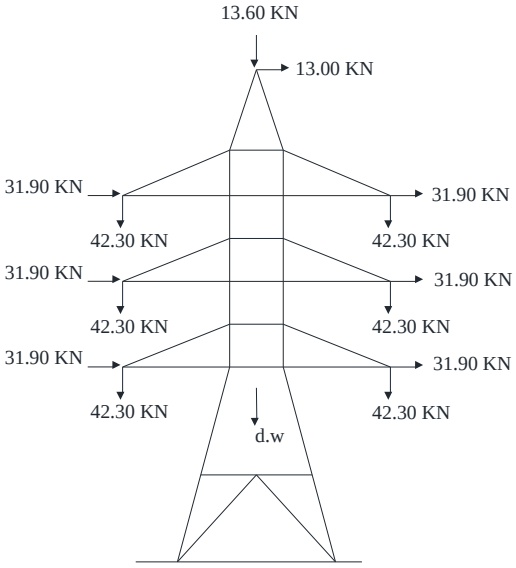

Load case description: 1.MAXIMUM ANGLE DRAWING
Case #: 13

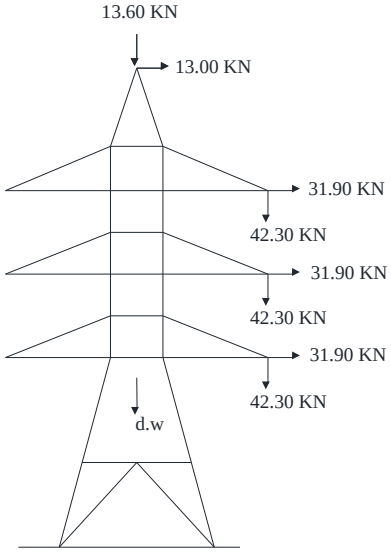

Load case description: 2.MAXIMUM ANGLE DRAWING
Case #: 14

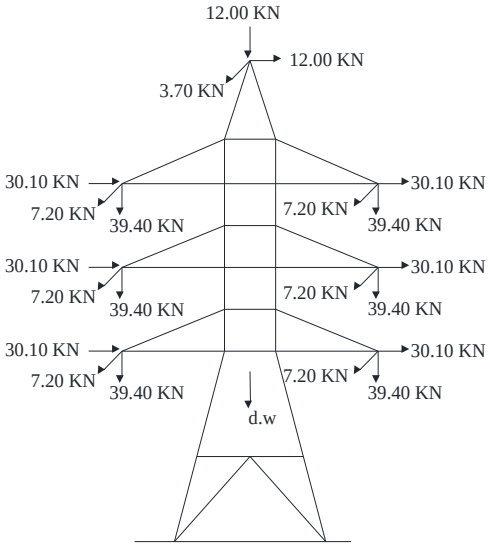

Load case description: 1.UNBALANCED ICING
Case #: 15

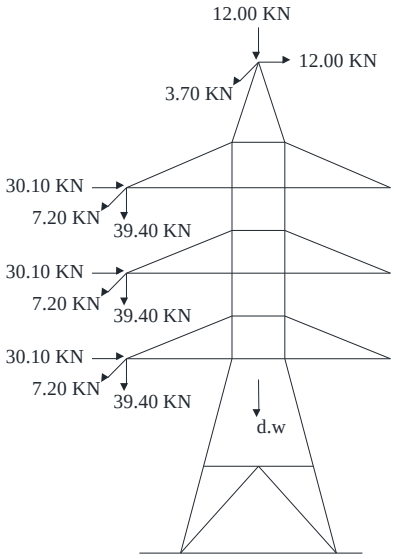

Load case description: 2.UNBALANCED ICINC
Case #: 16

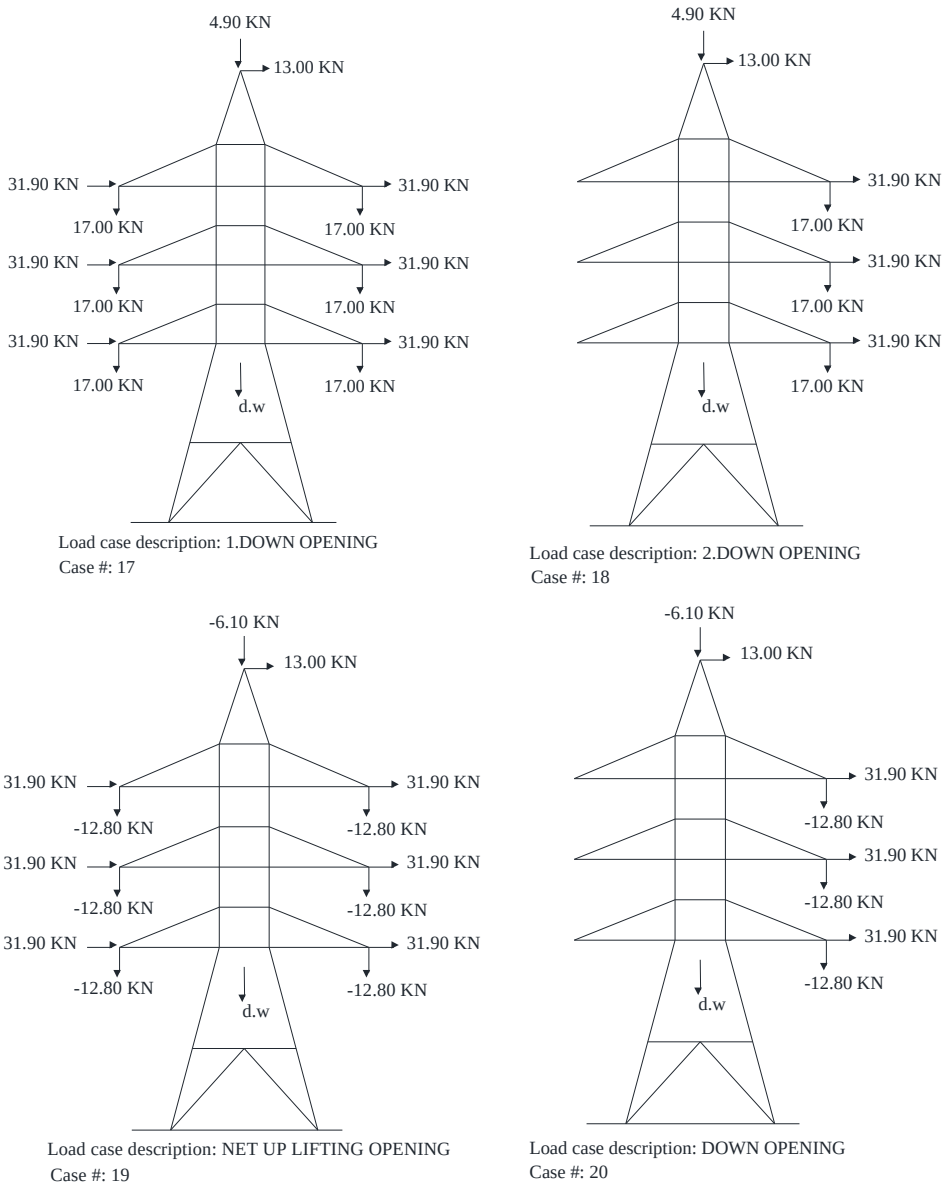

Figure 8. The details of the 20 load cases as combinations of different loads

3.5. Details of Seismic Parameters

The design spectrums created and scaled the ground motions. They were selected to fit the design spectrum within the duration of interest [20]. We should note that a place with high acceleration spectral values (e.g. Eskisehir Osmangazi University (ESOGU)) has been maintained as shown in Table 4.

Table 4. Identified locations and their respective seismic spectral values (site class ZA)

Province	Location	Seismic Data			
		(Ss)	(S1)	(PGA)	(PGV)
Eskisehir	ESOGU	0.703	0.186	0.298	17.934

This study used a set of ten ground motion registers from the Pacific Earthquake Engineering Research (PEER) Ground Motion Database (2019). In the current study, we take the time series with the greatest peak of ground acceleration for the horizontal component into account. We describe these ground motions data and parameters of concern for the structural dynamic analysis in Table 5, which presented the coefficients Fs and Fv specified in Turkey Earthquake Hazard Interactive Web Application for site class ZA. Table 6 presents 10 selected Earthquake records. Therefore, Figure 9 shows the acceleration-time diagrams of the selected records motions from PEER Ground Motion Database (2019).

Table 5. Coefficients Fs and Fv for site class ZA

Local Soil Effect Coefficient for the short period region, Fs					Local Soil Effect Coefficient for 1.0 second period, F1				
$S_S \leq 0.25$	$S_S = 0.50$	$S_S = 0.75$	$S_S = 1.00$	$S_S = 1.25$	$S_1 \leq 0.10$	$S_1 = 0.20$	$S_1 = 0.30$	$S_1 = 0.40$	$S_1 = 0.50$
0.8	0.8	0.8	0.8	0.8	0.8	0.8	0.8 `	0.8	0.8

Table 6. Earthquake records selected – horizontal component

Local Site Class: ZA					
Record No.	**Earthquake**	**Date**	**Station**	**Record Duration**	**Fault type**
P0856	Landers	28.06.1992	21081 Amboy	50	SS
P0969	Northridge	17.01.1994	24611 LA- Temple & Hope	40	RN
P0859	Landers	28.06.1992	32057 Baker Fire Sattion	50	SS
P1108	Kocaeli, Turkey	17.08.1999	Mecidiyekoy	44	SS
P0740	Loma Prieta	18.10.1989	57064 Fremont- Mission San Jose	39.9	RO
P0903	Northridge	17.01.1994	24157 LA – Baldwin Hills	40	RN
P0988	Northridge	17.01.1995	90009 N.Hollywood – Goldwater Can	21.9	RN
P1100	Kocaeli, Turkey	17.08.1999	Goyunk	25.5	SS
P0763	Loma Prieta	18.10.1989	1686 Fremont – Emerson Court	39.7	RO
P0818	Landers	28.06.1992	5070 North Palm Springs	70	SS

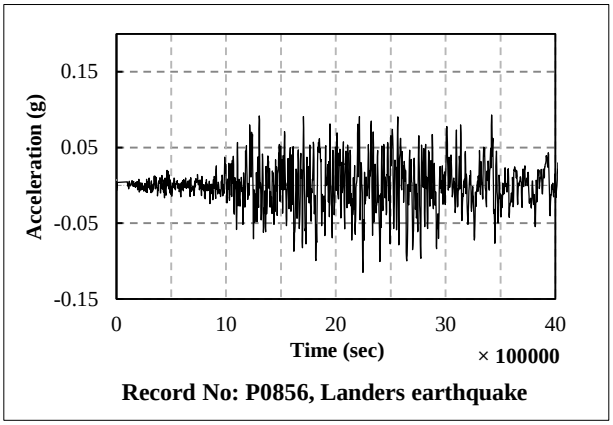

Record No: P0856, Landers earthquake

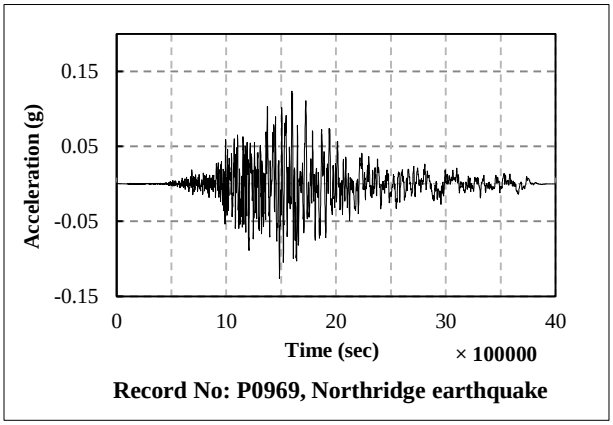

Record No: P0969, Northridge earthquake

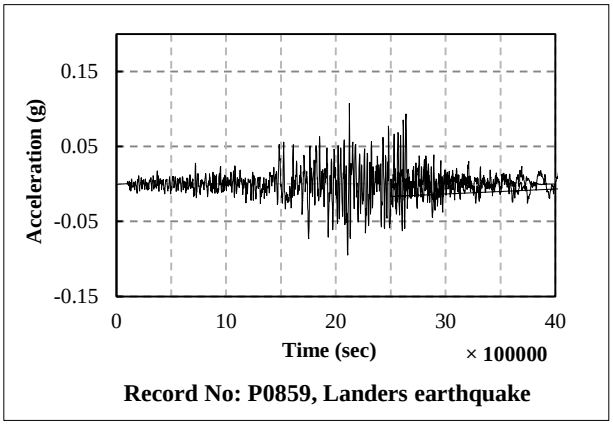

Record No: P0859, Landers earthquake

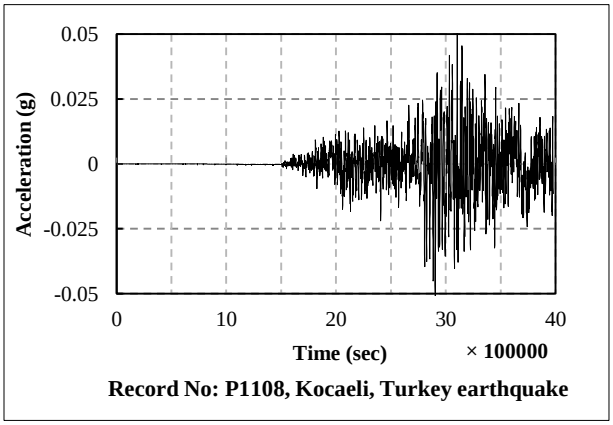

Record No: P1108, Kocaeli, Turkey earthquake

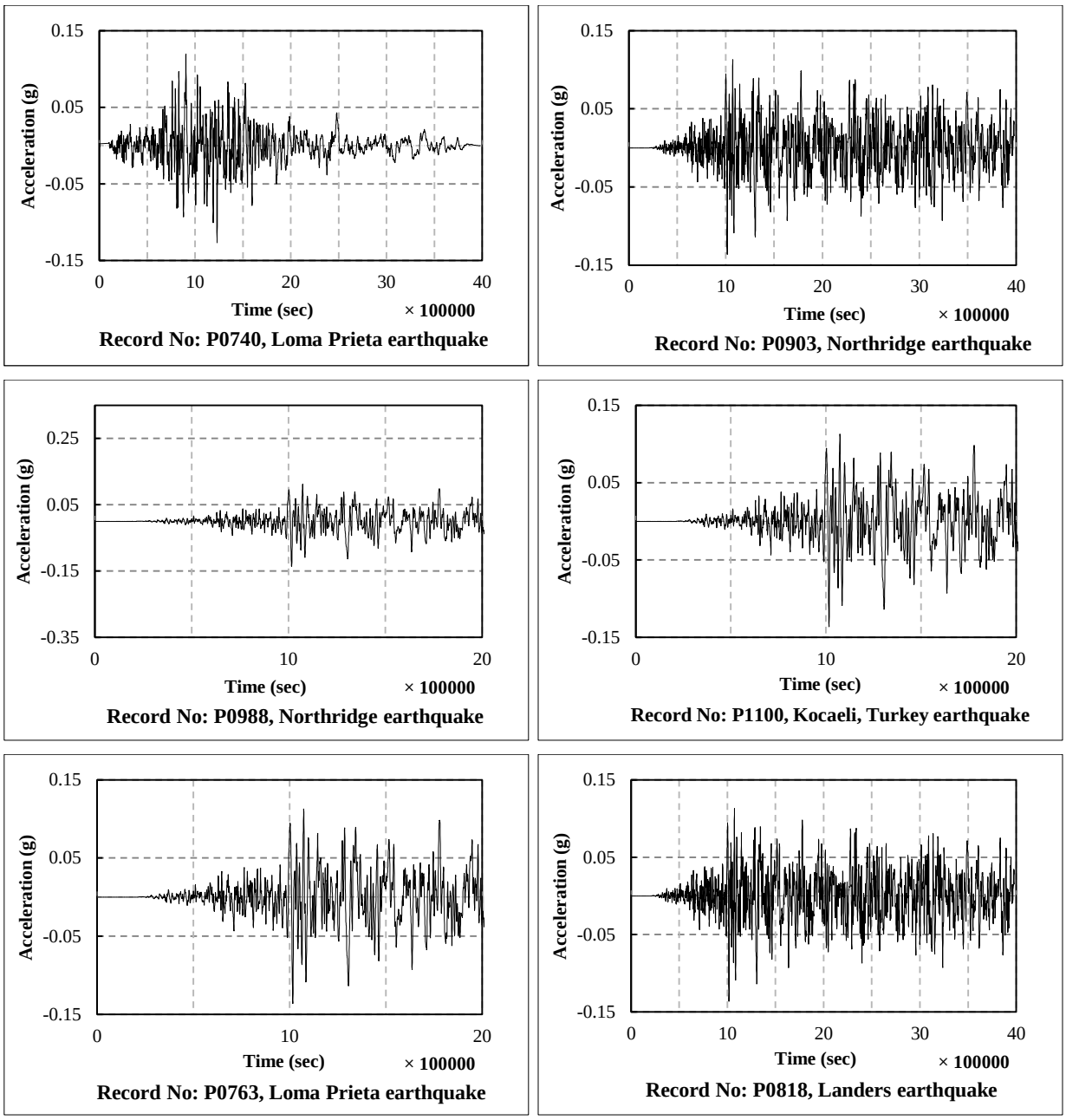

Figure 9. Acceleration- time diagrams of the motion of the selected record from PEER Ground Motion Database (2019)

Ten of those records are typical of soil class ZA which has a soil profile distinguished by dense soil and hard rock. Every record of the ground motions examined in the study has to be scaled for the sake of matching the defined design spectrum at the structural fundamental period (T1). Turkey Earthquake Building Code (TBDY-2018) provisions need that the mean of the 5% damped response spectra of ground motion records should match or be above the target spectra over the defined interval. According to TBDY-2018, the average of 5% damped for soil movement records over the defined interval must match or exceed the target spectra. Figure 10 shows the Horizontal Elastic Design Spectrum which was obtained from the following relationship:

Design Spectral Acceleration Coefficients

$S_{DS} = S_s F_s = 0.703 \times 0.8 = 0.562$

$S_{D1} = S_1 F_1 = 0.186 \times 0.8 = 0.149$

S_{DS} = Short period design spectral acceleration coefficient.

S_{D1} = 1.0 Design spectral acceleration coefficient for the second period.

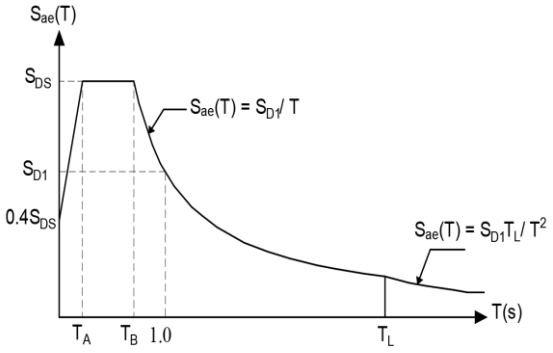

Related formulas:

$$S_{ae}(T) = \left(0.4 + 0.6\,\frac{T}{T_A}\right) S_{DS} \qquad (0 \le T \le T_A)$$

$$S_{ae}(T) = S_{DS} \qquad (T_A \le T \le T_B)$$

$$S_{ae}(T) = \frac{S_{D1}}{T} \qquad (T_B \le T \le T_L) \qquad (1)$$

$$S_{ae}(T) = \frac{S_{D1} T_L}{T^2} \qquad (T_L \le T)$$

$$T_A = 0.2\frac{S_{D1}}{S_{DS}}, \quad T_B = \frac{S_{D1}}{S_{DS}}, \quad T_L = 6s$$

$$T_A = 0.053(s), \quad T_B = 0.265(s), \quad T_L = 6.00(s)$$

S_{ae} = Design Spectral Response Acceleration.

T = The fundamental period of the structure (s).

T_L = Long-period transition period (s).

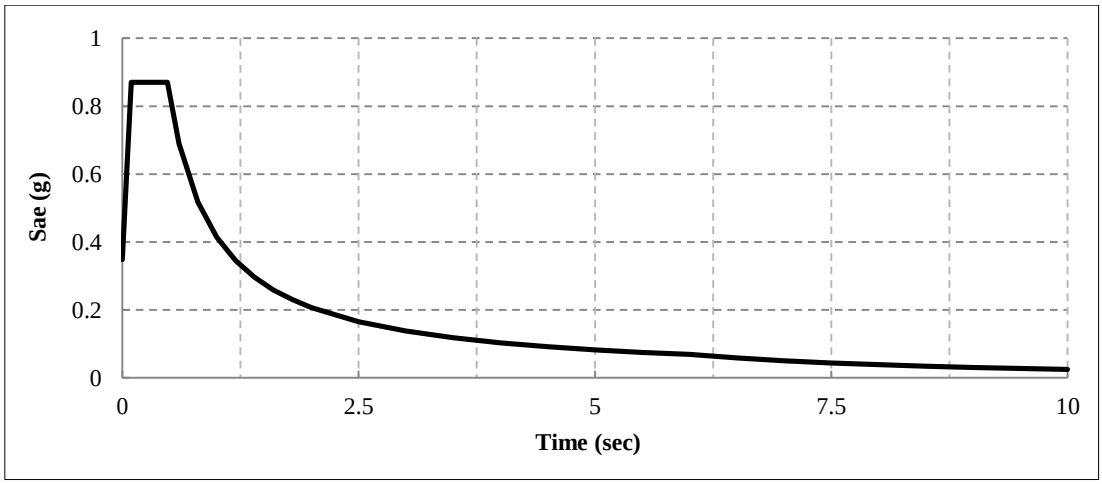

Figure 10. Horizontal Elastic Design Spectrum

The current study included this provision to scale the selected records of soil movement. Figure 11 shows the scale acceleration response spectrum of the ZA class. It has been noticed that only the frequency content was scaled for the acceleration response spectrum. Figure 12 presents the flowchart of the adopted method.

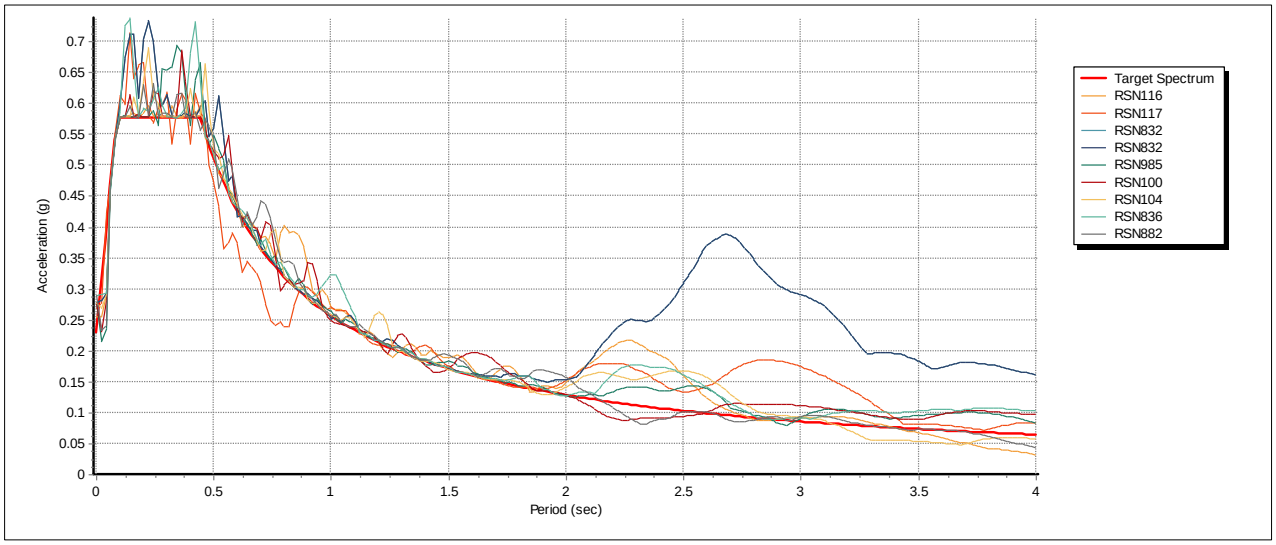

Figure 11. Design response spectrum for 5% damping, site Class ZA (TBDY-2018), and the response spectra of selected scaled records

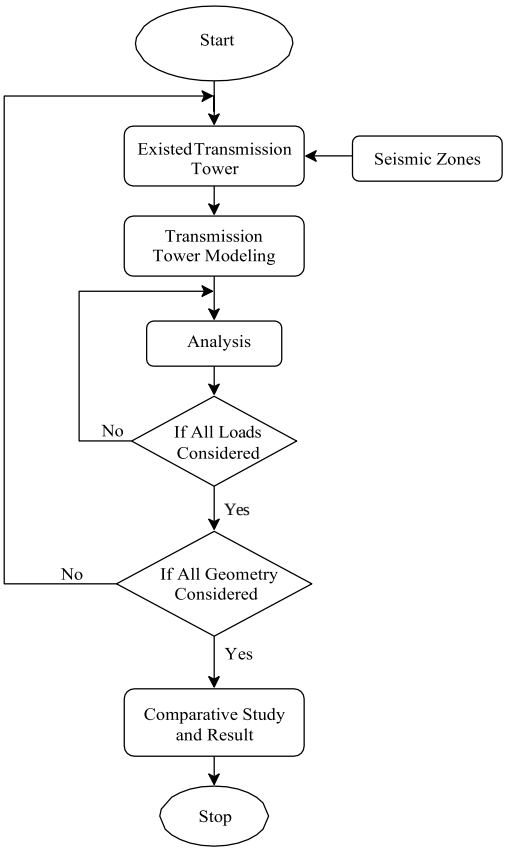

Figure 12. Flow chart of the adopted methodology

4. Results

4.1. Natural Frequency Analysis

We carry out the model analysis for the design using the eigenvector method. Once directing the modular analysis, it is guaranteed that the outcomes incorporate a sufficient degree of structural mass that has been done by remembering enough modes for the analysis to catch 90% of the mass participation at every one of the three displacement directions. The mass participation proportion shows the level of the basic mass for the model taking part in providing guidance and mode. It appears in Table 7 that mode 330 is achieved.

Table 7. Modal mass participation ratios

Mode No. (-)	Participation mass ratio (%)					
	UX	UY	UZ	SumUX	SumUY	SumUZ
1	0.000	0.520	0.000	0.000	0.520	0.000
2	0.536	0.000	0.000	0.536	0.520	0.000
3	0.000	0.000	0.000	0.536	0.521	0.000
4	0.000	0.237	0.000	0.536	0.757	0.000
5	0.000	0.000	0.001	0.536	0.757	0.001
6	0.250	0.000	0.000	0.786	0.757	0.001
7	0.000	0.000	0.002	0.786	0.757	0.003
8	0.000	0.000	0.000	0.786	0.757	0.003
9	0.000	0.000	0.000	0.786	0.757	0.003
10	0.000	0.000	0.008	0.786	0.757	0.011
11	0.000	0.005	0.000	0.786	0.763	0.011
25	0.019	0.009	0.000	0.920	0.867	0.019
150	0.000	0.000	0.000	0.991	0.991	0.704
239	0.000	0.000	0.000	0.994	0.994	0.827
330	0.000	0.000	0.001	0.996	0.995	0.900

Table 8 shows the modal periods and natural frequencies of the modes listed in Table 7.

Table 8. Modal periods and natural frequencies of the tower

Mode No.	Period (s)	Frequency (Hz)	Shape
1	0.410	2.434	Longitudinal
2	0.400	2.500	Transversal
3	0.133	7.517	Torsion
4	0.123	8.123	Longitudinal
5	0.118	8.456	Vertical
6	0.114	8.756	Transversal
7	0.088	11.326	Vertical
8	0.088	11.328	Vertical
9	0.088	11.329	Vertical
10	0.071	13.978	Vertical
11	0.0686	14.578	Longitudinal
25	0.059	16.852	Transversal
150	0.019	53.730	Vertical
239	0.012	81.652	Longitudinal
330	0.008	120.940	Vertical

As it should be with any mode in which the mode shape is longitudinal, transverse or vertical head, this mode is caused by the corresponding direction of displacement. For torsional shaped, mass participation in all directions is zero. We estimate the response of the structure by the initial four transverse and longitudinal modes.

Here, we separate transverse mode shapes for actual interest as we use the high dynamic wind load in this direction. The four modes 2, 6, 20, and 25 are shown in Figures 13 to 16 where their mass participation is higher than 1%for the direction of transverse. Point out that we show the figures in their easiest 'wireframe' form for clarification owing to the structure's height. Therefore, the figures have also been scaled to show the mode forms better.

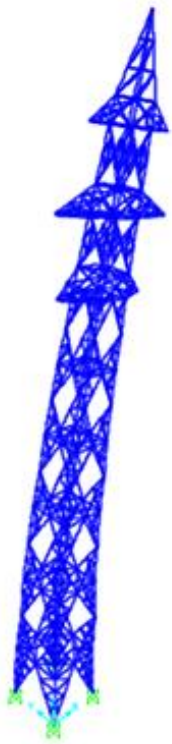

Figure 13. Mode 2 - frequency= 2.500 Hz

Figure 14. Mode 6 – frequency = 8.756Hz

Figure 15. Mode 20 – frequency = 16.521 Hz

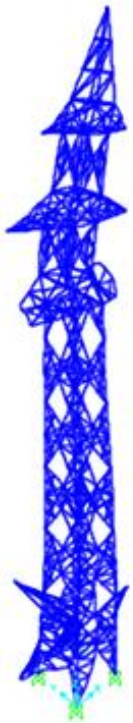

Figure 16. Mode 25– frequency = 16.852 Hz

4.2. Design using AISC 360-16 Code

The study has been carried out using SAP2000 that can perform both static and dynamic analysis as well as using necessary combinations. In this study, the AISC360-16 code, which is the most suitable for Turkey earthquake building code (TBDY-2018), has been used.

Load cases are a set of load and boundary conditions used to define particular loading conditions. In the study, we have taken the load cases which have been used to study the linear response from a structure subjected to different loading conditions from Turkey Electricity Distribution (TEDAS).

4.3. Design with the Same Sections Which Have Been Taken From TEDAS

We designed the section members of the transmission tower. Therefore, several sections have not passed as seen in Figure 17. 18 steel frames failed the stress/capacity check as illustrated in Table 9, which provides the summary data for the designed frames used in the current work.

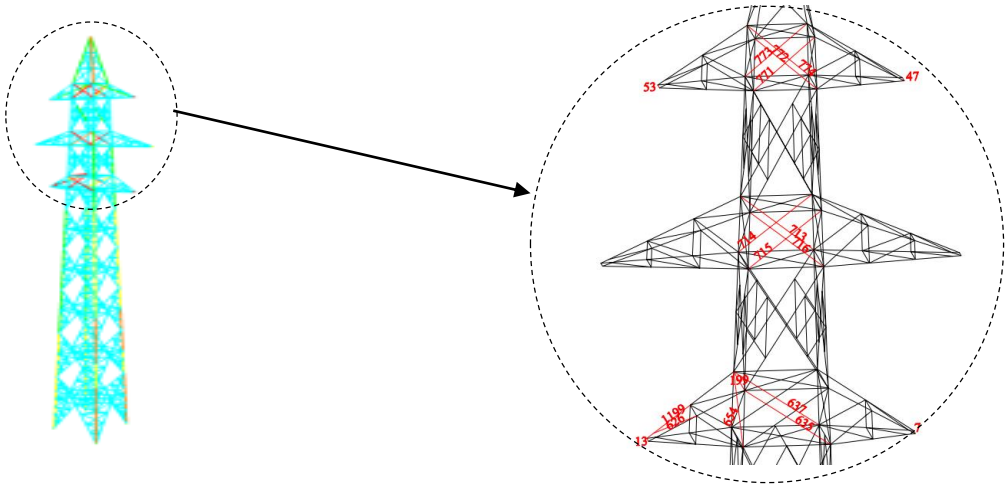

Figure 17. The failed sections of the transmission tower

Table 9. Steel Design - Summary Data - AISC 360-16

Frame No.	Design Section	Ratio	Combo
7	L80X7	1.82	COMB1
13	L80X7	1.98	COMB2
47	L80X10	1.35	COMB1
53	L80X10	1.76	COMB2
199	L70X7	1.15	COMB11
626	L60X5	1.69	COMB2
635	L80X7	1.08	COMB1
637	L80X7	1.08	COMB11
654	L80X7	1.17	COMB2
713	L70X7	1.41	COMB14
714	L70X7	1.08	COMB2
715	L70X7	0.95	COMB2
716	L70X7	1.43	COMB10
771	L50X5	1.96	COMB2
772	L50X5	2.52	COMB14
773	L50X5	2.11	COMB2
774	L50X5	2.52	COMB14
1199	L60X6	12.73	COMB2

4.4. Modeling and Parametric Analysis of Bolted Connections on Retrofitted Transmission Tower Members

The useful retrofitting method for attaching parallel reinforcement components to critical members (Figure 18) has been used on transmission line towers in Turkey and worldwide.

Figure 18. Method of retrofitting

In this approach, a critical leg component and parallel reinforcement members are connected by cross-shaped bolt connections (Figure 19.a). The cross-shaped connections transfer large external loads from the critical legs member of the reinforcement components so that less loads transport in critical legs and they increase the total load carrying the amount that can be contained. Splicing joints (Figure 19. b) are used in grid transmission towers to connect the critical lengths of leg members. Therefore, cruciform and joint connections are significant factors within the structural behavior of the legs of retrofitted transmission towers.

(a) Cruciform connection **(b) splice joint**

Figure 19. Connection of transmission tower

Experimental investigation in the joint connections provided the concept of "slip resistance" relying on a set of effecting factors, for instance, bolt arrangement, properties of the material surface, material strength, and torque values.

Relying on this study, 'Ungkurapinan et al. (2003)' carried out experimental research on the load transfer behavior of screw connections with the same steel angles. In this work, we developed experimental and theoretical expressions of the load shift. We then used this load switching behavior for screw connections in the fault analysis of network towers [21].

Studies on cross-connections have been carried out too. Experimental research showed that the load transfer behavior of cross-connections depends on the screw arrangement. 'Zhuge et al. (2012)' has extended these research results from the numerical analysis [22]. 'Mills et al. (2012)' also suggested a retrofitted powerline tower test. Moreover, he concluded that the cross-connection in a transmission tower system has sufficient load transmission capability.

However, the influencing variables and error paths of the combination of cross and joint connections have not been examined. Therefore, the authors have investigated the load transfer behavior of cross-connections and joints using experimental tests and compared the results with models that were developed in software called ABAQUS. They then carried out a parametric study, taking into account friction coefficients, screw numbers, and torque values using the confirmed numerical models [23].

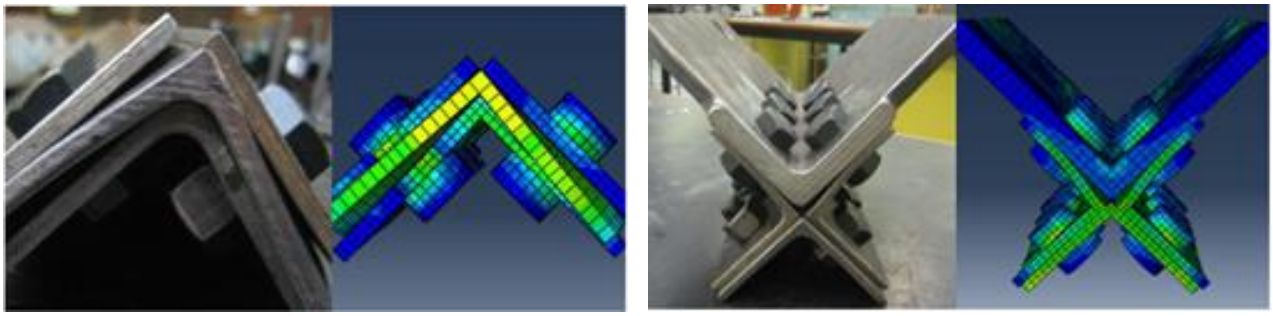

(a) 12 blot cruciform joints **(b) 12 blot splice joints**

Figure 20. The failure mode of specimens (CTC type)

Lu et al. (2014) presented in their study the load shifting behavior of the cross and joint connections to the legs of retrofitted gear towers. ABAQUS has been used for designing numerical models to make a pretense of experimental tests and in a parametric study, then they used the number of verified models. Depending on both the experimental and numerical test results, they found the assembly specification affecting the load shifting behavior, Figure 20, displays failure mode of CTC section type [24].

4.5. Replace the Failed Sections in the Tower with New Sections

In our study, we replaced the failed sections with the CTC section type. Figure 21 presents the section designed with SAP2000 software. The comparative data summary of the designed steel using AISC 360-16 is highlighted in Table 10.

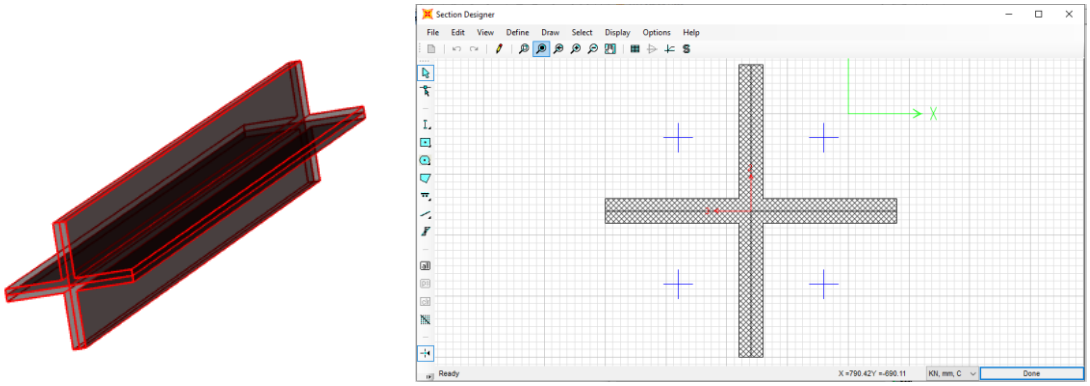

Figure 21. The newly designed section in SAP2000

Table 10. Comparative of Steel Design -Summary Data - AISC 360-16

Frame No.	Design Section	Ratio	Replaced section	Ratio
7	L80X7	1.82	CTC 80x7	0.58
13	L80X7	1.98	CTC 80x7	0.56
47	L80X10	1.35	CTC 80x10	0.41
53	L80X10	1.76	CTC 80x10	0.61
199	L70X7	1.15	CTC 70x7	0.10
626	L60X5	1.69	CTC 60x5	0.21
635	L80X7	1.08	CTC 80X7	0.10
637	L80X7	1.08	CTC 80X7	0.10
654	L80X7	1.17	CTC 80X7	0.10
713	L70X7	1.41	CTC 70X7	0.10
714	L70X7	1.08	CTC 70X7	0.10
715	L70X7	0.95	CTC 70X7	0.50
716	L70X7	1.43	CTC 70X7	0.08
771	L50X5	1.96	CTC 50X5	0.10
772	L50X5	2.52	CTC 50X5	0.09
773	L50X5	2.11	CTC 50X5	0.07
774	L50X5	2.52	CTC 50X5	0.09
1199	L60X6	12.73	CTC 60X6	0.40

5. Conclusions

The seismic study of transmission towers in Turkey developed a set of time history analyses using non-linear finite element (FE) models on towers and a set of 10 recorded earthquake ground motions. We shall conclude that the designed transmission towers are not safe from earthquakes in Turkey.

For the 154 kV transmission towers, the buckling developed in the steel members is further probable to occur to steel sections in the cage (top part) of the towers. A relationship has been determined between the transmission tower height and the seismic vulnerability for transmission towers.

The results show that the load of failure increased after retrofitting. The retrofitting method was effective and easy to be conducted in fields. Disadvantages of the current research, which are the effect of connection design parameters, bolt arrangement, properties of the material surface, material strength, and torque values, on the connection model, have not been discussed.

Potential improvements on the study are as follows; i) We can use a transmission tower more than once, also we should do an optimization study to keep the weight as low as possible; ii) Analysis and design of the transmission tower can be carried out by different engineering softwares, then comparison will lead us to the best results; iii) For a more accurate examination of the seismic performance of the transmission towers, a non-linear time-history analysis considering the interaction of soil-structure will be required.

6. Acknowledgement

Authors would like to express special thanks to “Türkiye Scholarships” which is a government-funded, competitive scholarship program, awarded to outstanding students and researchers to pursue full-time or short-term program at the top universities in Turkey. Authors would also like to thanks to TEDAS (Turkish Electricity Distribution Corporation) to share technical drawings and details of transmission towers.

7. Conflicts of Interest

The authors declare no conflict of interest.

8. References

[1] Rajoriya, Sourabh, K. K. Pathak, and Vivekanand Vyas. "Analysis of Transmission Tower for Seismic Loading Considering Different Height and Bracing System." International Journal for Research in Applied Science & Engineering Technology, ISSN (2016): 2321-9653.

[2] Karthik, Siddu, and G. V. Sowjanya. "Static and Dynamic Analysis of Transmission Line Towers under Seismic Loads." International journal of engineering research and technology 4 (08) (2015): 29-33. doi: 10.17577/ijertv4is080118.

[3] Albayrak, Uğur, Mehmet Canbaz, and Gülçağ Albayrak. "A rapid seismic risk assessment method for existing building stock in urban areas." Procedia engineering 118 (2015): 1242-1249. doi:10.1016/j.proeng.2015.08.476.

[4] Tian, Li, Liulu Guo, Ruisheng Ma, Xia Gai, and Wenming Wang. "Full-scale tests and numerical simulations of failure mechanism of power transmission towers." International Journal of Structural Stability and Dynamics 18, no. 09 (2018): 1850109. doi:10.1142/s0219455418501092.

[5] Tian, Li, Haiyang Pan, Ruisheng Ma, Lijuan Zhang, and Zhengwei Liu. "Full-scale test and numerical failure analysis of a latticed steel tubular transmission tower." Engineering Structures 208 (2020): 109919. doi:10.1016/j.engstruct.2019.109919.

[6] Park, Hyo-Sang, Byung Ho Choi, Jung Joong Kim, and Tae-Hyung Lee. "Seismic performance evaluation of high voltage transmission towers in South Korea." KSCE Journal of Civil Engineering 20, no. 6 (2016): 2499-2505. doi:10.1007/s12205-015-0723-3.

[7] YÜKSEL, İsa. "An Overview on Tall Buildings from the Point of Structural Engineering." Journal of Innovative Science and Engineering (JISE) 3, no. 2 (2019): 86-101. doi:10.38088/jise.590738.

[8] Pan, Haiyang, Li Tian, Xing Fu, and Hongnan Li. "Sensitivities of the seismic response and fragility estimate of a transmission tower to structural and ground motion uncertainties." Journal of Constructional Steel Research 167 (2020): 105941. doi:10.1016/j.jcsr.2020.105941.

[9] Tian, Li, Juncai Liu, Canxing Qiu, and Kunjie Rong. "Temperature effect on seismic behavior of transmission tower-line system equipped with SMA-TMD." Smart Structures and Systems 24, no. 1 (2019): 1-14.

[10] Tian, Li, Ruisheng Ma, and Bing Qu. "Influence of different criteria for selecting ground motions compatible with IEEE 693 required response spectrum on seismic performance assessment of electricity transmission towers." Engineering Structures 156 (2018): 337-350. doi:10.1016/j.engstruct.2017.11.046.

[11] Zheng, Hua-Dong, and Jian Fan. "Analysis of the progressive collapse of space truss structures during earthquakes based on a physical theory hysteretic model." Thin-Walled Structures 123 (2018): 70-81. doi:10.1016/j.tws.2017.10.051.

[12] Tian, Li, Haiyang Pan, and Ruisheng Ma. "Probabilistic seismic demand model and fragility analysis of transmission tower subjected to near-field ground motions." Journal of Constructional Steel Research 156 (2019): 266-275. doi:10.1016/j.jcsr.2019.02.011.

[13] Wu, Ruo-Yang, and Chris P. Pantelides. "Seismic evaluation of repaired multi-column bridge bent using static and dynamic analysis." Construction and Building Materials 208 (2019): 792-807. doi:10.1016/j.conbuildmat.2019.03.027.

[14] Moon, Byoung-Wook, Ji-Hun Park, Sung-Kyung Lee, Jinkoo Kim, Taejin Kim, and Kyung-Won Min. "Performance evaluation of a transmission tower by substructure test." Journal of Constructional Steel Research 65, no. 1 (2009): 1-11. doi:10.1016/j.jcsr.2008.04.003.

[15] Alam, M. J., and A. R. Santhakumar. "Reliability analysis and full-scale testing of transmission tower." Journal of Structural Engineering 122, no. 3 (1996): 338-344. doi:10.1061/(asce)0733-9445(1996)122:3(338).

[16] American Society of Civil Engineers Task Committee on Tower Design. "Guide for design of steel transmission towers." American Society of Civil Engineers, 1971.

[17] Lei, Y. H., and Y. L. Chien. "Seismic analysis of transmission towers under various line configurations." Structural Engineering and Mechanics 31, no. 3 (2009): 241-264. doi:10.12989/sem.2009.31.3.241.

[18] Chen, Bo, Wei-hua Guo, Peng-yun Li, and Wen-ping Xie. "Dynamic responses and vibration control of the transmission tower-line system: a state-of-the-art review." The Scientific World Journal 2014 (2014). doi:10.1155/2014/538457.

[19] Da Silva, J. G. S., PCG Da S. Vellasco, S. A. L. De Andrade, and M. I. R. De Oliveira. "Structural assessment of current steel design models for transmission and telecommunication towers." Journal of Constructional Steel Research 61, no. 8 (2005): 1108-1134. doi:10.1016/j.jcsr.2005.02.009.

[20] De Macedo, Rodrigo. "Seismic Response of Transmission Line Guyed Towers With and Without the Interaction of Tower Conductor Coupling." PhD diss., Concordia University, 2016.

[21] Ungkurapinan, N., SR De S. Chandrakeerthy, R. K. N. D. Rajapakse, and S. B. Yue. "Joint slip in steel electric transmission towers." Engineering Structures 25, no. 6 (2003): 779-788. doi:10.1016/s0141-0296(03)00003-8.

[22] Zhuge, Yan, Julie E. Mills, and Xing Ma. "Modelling of steel lattice tower angle legs reinforced for increased load capacity." Engineering structures 43 (2012): 160-168. doi:10.1016/j.engstruct.2012.05.017.

[23] Lu, Chenghao, Xing Ma, and Julie E. Mills. "Modelling and parametric analysis of bolted connections on retrofitted transmission tower leg members." (2014): 571. doi:10.1061/9780784479414.039.

[24] Lu, Chenghao, Xing Ma, and Julie E. Mills. "The structural effect of bolted splices on retrofitted transmission tower angle members." Journal of Constructional Steel Research 95 (2014): 263-278. doi:10.1016/j.jcsr.2013.12.011.